SUPPLEMENTARY INFORMATION

Swelling behavior of the L_α phase

Variation of the lamellar periodicity with Φ_s in the L_α phase is shown in figure 1. The maximum water content of the L_α phase is found to be about 35 wt% beyond which it coexists with excess water forming a MLV dispersion. Within the narrow composition range where the pure L_α phase exists, variation of the lamellar periodicity (d) follows the expected swelling behavior given by $d = \delta/\phi$, where δ is the bilayer thickness and ϕ the amphiphile volume fraction, with $\delta = 2.49$ nm. Here we have assumed the density of the bilayer to be 1, so that $\phi = \Phi_s$.

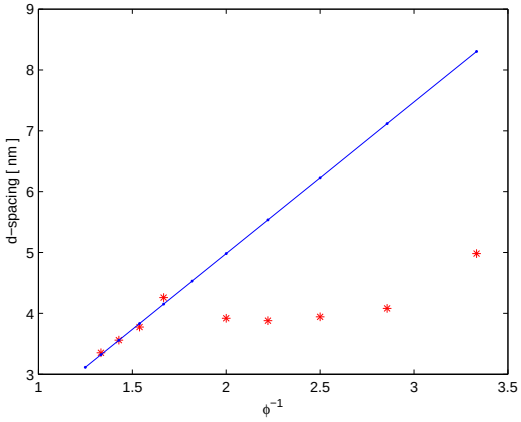

FIG. 1: Swelling behavior of the lamellar phase of the SDS-PTHC-water system at T = 25 °C and $\alpha = 1$.

Analysis of the SAXS data

The SAXS patterns were analyzed following the procedure described in ref. [1]. The scattered intensity is given by

$$I(q) = S(q)|F(q)|^2/q^2 + N_u|F(q)|^2/q^2, \tag{1}$$

where S(q) is the structure factor and F(q) the form factor of the bilayers. F(q) is given by the Fourier transform of the bilayer electron density profile $\rho(z)$. $\rho(z)$ is modeled as consisting of two Gaussians of width σ_h representing the headgroups, centered at z = ± z_h, and a third Gaussian of width σ_c at the bilayer center(z = 0) representing the terminal methyl groups,

$$\rho(z) = \rho_{CH_2} + \bar{\rho}_h[exp(-\frac{(z-z_h)^2}{2\sigma_h^2} + exp(-\frac{(z+z_h)^2}{2\sigma_h^2}) + \bar{\rho}_c(exp - \frac{z^2}{2\sigma_c^2})], \tag{2}$$

where the electron densities of the headgroup $\bar{\rho}_h$ and hydrocarbon tails $\bar{\rho}_c$ are defined relative to the methylene electron density ρ_{CH_2}.

The second term in eqn.1 is due to diffuse scattering from uncorrelated bilayers and is needed when uncorrelated bilayers coexist with a lamellar phase, with N_u giving their relative concentration.

The structure factor of the lamellar stack is given by [1, 2],

$$S(q) = N + 2\sum_{k=1}^{N-1}(N-k)cos(kqd) \times e^{-(d/2\pi)^2q^2\eta\gamma}(\pi k)^{-(d/2\pi)^2q^2\eta} \tag{3}$$

N is the mean number of coherent scattering bilayers in the stack and γ the Eulers' constant. The Caille parameter $\eta = q^2k_BT/(8\pi\sqrt{KB})$, where k_B is the Boltzmann constant, T the temperature, K and B the bending and bulk moduli of the lamellar phase.

Table 1 gives the variation of the model parameters across the UB $\rightarrow$ L_i transition at $\alpha = 1.0$ and $\Phi_s = 30$ wt%. The corresponding SAXS patterns along with the fits to the above model are given in fig. 2a in the text. The bilayer electron density profiles, obtained from the model, are shown in fig. 2b.

Table 2 gives similar data for the $L_\alpha \rightarrow L_i$ transition at $\alpha = 1.1$ and $\Phi_s = 20$ wt%. The corresponding SAXS patterns and bilayer electron density profiles are shown in figs. 2c and 2d in the text.

The SAXS patterns of the UB phase can be accounted for with just the bilayer form factor (second term in eqn.1), showing that the bilayers in this phase are positionally uncorrelated. On the other hand, only the first term is required in the case of the L_α and L_i phases. The number of correlated bilayers in the L_α phase is $\sim$ 10 whereas in the L_i phase it is $\sim$ 2. Values of all other model parameters are comparable in the three phases. Thus the SAXS data are consistent with the L_i phase being made up of bilayers, just as the L_α phase, but with positional correlations extending over only 2 - 3 bilayers.

T ($^\circ C$)	80	85	90
Phase	UB	UB	L_i
z_H (nm)	0.89 $\pm$ 0.06	0.96 $\pm$ 0.05	1.02 $\pm$ 0.05
σ_H (nm)	0.46 $\pm$ 0.06	0.40 $\pm$ 0.05	0.48 $\pm$ 0.00
σ_C (nm)	0.79 $\pm$ 0.03	0.75 $\pm$ 0.06	0.46 $\pm$ 0.06
$\overline{\rho_C}/\overline{\rho_H}$	-1.19 $\pm$ 0.11	-1.09 $\pm$ 0.06	-1.95 $\pm$ 0.23
d (nm)	–	–	4.33 $\pm$ 0.04 *
η_1	–	–	1.31 $\pm$ 0.06 †
N	–	–	2 $\pm$ 0
N_u	–	–	0

TABLE I: Variation of the model parameters with temperature across the UB $\rightarrow$ L_i transition at $\alpha = 1.0$ and $\Phi_s = 30$ wt%. $*$ this corresponds to the average spacing in the L_i phase. † the larger value of this parameter should not be attributed to a lowering of the elastic moduli as in the case of the L_α phase, since the disorder in this phase is not of thermal origin, but is due to defects.

T ($^\circ C$)	75	80	85	90
Phase	L_α	L_α	L_i	L_i
z_H (nm)	0.87 $\pm$ 0.05	0.83 $\pm$ 0.09	0.93 $\pm$ 0.01	0.93 $\pm$ 0.01
σ_H (nm)	0.46 $\pm$ 0.04	0.46 $\pm$ 0.07	0.40 $\pm$ 0.01	0.48 $\pm$ 0.01
σ_C (nm)	0.78 $\pm$ 0.03	0.71 $\pm$ 0.08	0.6 $\pm$ 0.1	0.6 $\pm$ 0.1
$\overline{\rho_C}/\overline{\rho_H}$	-1.13 $\pm$ 0.08	-1.24 $\pm$ 0.08	-1.3 $\pm$ 0.2	-1.4 $\pm$ 0.2
d (nm)	6.67 $\pm$ 0.01	6.68 $\pm$ 0.01	4.30 $\pm$ 0.06 *	4.35 $\pm$ 0.05 *
η_1	0.57 $\pm$ 0.02	0.56 $\pm$ 0.02	1.46 $\pm$ 0.05 †	1.36 $\pm$ 0.05 †
N	8 $\pm$ 2	9 $\pm$3	2 $\pm$ 1	2 $\pm$ 1
N_u	0	0	0	0

TABLE II: Variation of the model parameters with temperature across the $L_\alpha \rightarrow L_i$ transition at $\alpha = 1.1$ and $\Phi_s = 20$ wt%. $*$ this corresponds to the average spacing in the L_i phase. † the larger value of this parameter should not be attributed to a lowering of the elastic moduli as in the case of the L_α phase, since the disorder in this phase is not of thermal origin, but is due to defects.

[1] G. Pabst, M. Rappolt, H. Amenitsch, and P. Laggner, Phys. Rev. E 62, 4000, 2000.
[2] R. Zhang, R. M. Suter and J. F. Nagle, Phys. Rev. E **50**, 5047, 1994.